

UNCLASSIFIED

Defense Technical Information Center
Compilation Part Notice

ADP012487

TITLE: Optimizing a Slingatron-Based Space Launcher Using MATLAB

DISTRIBUTION: Approved for public release, distribution unlimited

This paper is part of the following report:

TITLE: 10th U.S. Army Gun Dynamics Symposium Proceedings

To order the complete compilation report, use: ADA404787

The component part is provided here to allow users access to individually authored sections of proceedings, annals, symposia, etc. However, the component should be considered within the context of the overall compilation report and not as a stand-alone technical report.

The following component part numbers comprise the compilation report:

ADP012452 thru ADP012488

UNCLASSIFIED

OPTIMIZING A SLINGATRON-BASED SPACE LAUNCHER USING MATLAB[®]

M. Bundy¹, G. Cooper², S. Wilkerson³

¹*U.S. Army Research Laboratory, Aberdeen Proving Ground, MD 21005*

²*U.S. Army Research Laboratory, Aberdeen Proving Ground, MD 21005*

³*U.S. Army Research Laboratory, Aberdeen Proving Ground, MD 21005*

A slingatron is the name given to a propellantless mechanical means of launching a projectile. To date, slingatrons are only conceptual in nature, but their potential use as a ground-to-space launch mechanism for unmanned payloads is under investigation. Slingatrons can be configured in a variety of geometries; one form consists of a spiral track (or launch tube) that gyrates at a constant frequency about a set radius. Under proper conditions (design parameters), a projectile entering the spiral at its small-radius end will undergo nearly constant tangential acceleration before exiting. The differential equations governing the motion of the projectile within the spiral are highly non-linear, making the optimum design solution non-intuitive. This report describes how the slingatron works from first principles, then uses the numerical integration procedures within the computer software environment of Simulink[®] and MatLab[®] to search for and identify the optimum design solution parameters based on structural dynamics and mechanical design considerations.

PURPOSE OF STUDY

The cost of launching payloads into space is currently around \$10,000 per pound. Although this expense may be acceptable for manned space missions, it can be a curtailing financial burden for other potential enterprises. Less expensive, alternative methods of launching acceleration-insensitive bulk items into space is thus an area of interest. The slingatron is a proposed (propellantless) means of launching objects for such missions (Tidman et al. [1], Tidman [2,3], Tidman and Greig [4]). This study describes the operational principles of the slingatron and investigates the range of possible design solutions using Matlab and Simulink software; thus, bounding the physical scale of this mechanical device.

OPERATIONAL PRINCIPLES OF A SLINGATRON LAUNCHER

Those who played with a hoola-hoop as a child, and remember how the sound of the ball's speed within the hoop increased with the gyration rate of the hips, might recognize the similarity with a projectile in a slingatron. Figures 1–3 show the progression of forces in action in going from uniform circular motion to circular slingatron (or, hoola-hoop-type) motion. Specifically, Fig 1 displays uniform circular motion of a ball of mass m about a circle of radius D , with velocity \vec{v} , and centripetal force \vec{F}_D (all of constant magnitude).

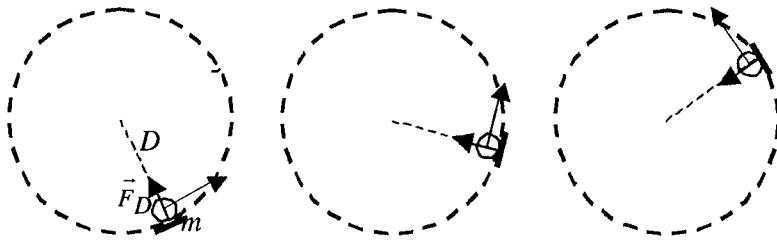


FIGURE 1. Uniform Circular Motion.

The speed of the ball in Fig 1 can be increased by orienting the normal force acting on the ball so that it has a tangential as well as a centripetal component. This could be done by envisioning a rotating wedge as shown in Fig 2. As the circular speed of the ball increases under the tangential force, so too must the angular velocity of the supporting wedge, as well as the normal force of the wedge on the ball, illustrated in Fig 2. (Note, if γ in Fig 2 is positive, the speed will increase; if γ is negative, it decreases; and when $\gamma = 0$, the speed stays constant, equivalent to Fig 1).

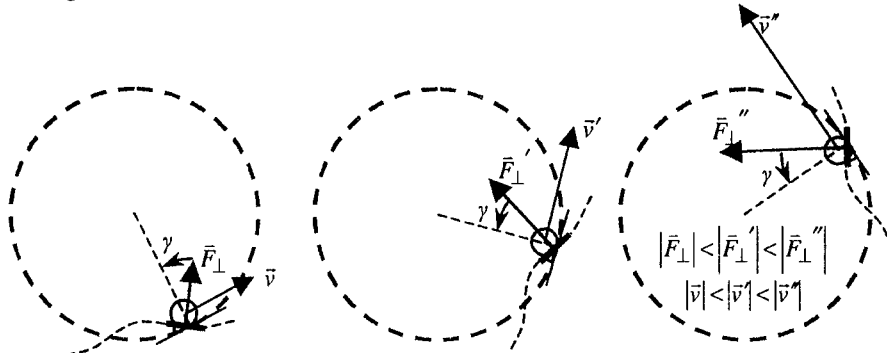


FIGURE 2. Non-Uniform Circular Motion Created by the Tangential Force Component of a Rotating Wedge (or Wave).

The effect of the rotating wedge (or wave) on mass m in Fig 2 can be duplicated by employing a gyrating ring of radius R , and therein lies the operational principle of the circular slingatron (or hoola-hoop), as shown in Fig 3. As indicated in the illustration, the gyrating ring can provide the same boundary geometry and normal force as the wedge. Like the wedge, the frequency of gyration, ψ , must increase in order for the ring to maintain its support for, stay in phase with, the object.

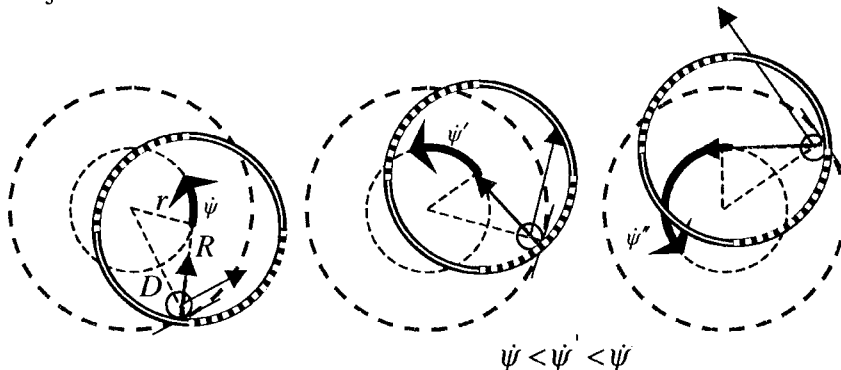


FIGURE 3. Non-Uniform Circular Motion Created by a Gyrating Ring.

In addition to the hoola-hoop, Fig 4a, swirling liquid in a cup by moving the hand in a circular pattern (oxidizing wine in glass, for instance) is another practical example, Fig 4b, of the same effect. In this case, the wave in the fluid moves up and around the sides of the cup/glass. (As a practical exercise, hand swirling liquid in a cup reveals how important the gyration phase angle is to maintaining, or increasing, the wave speed/amplitude.)

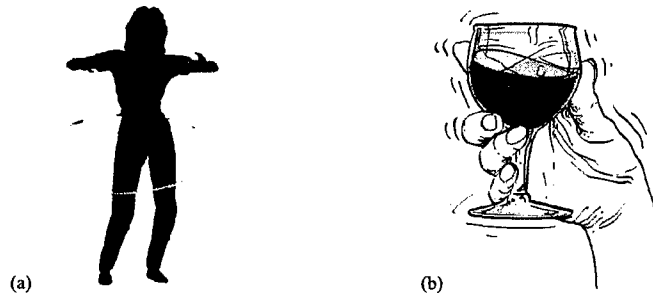


FIGURE 4. Slingatron-Like Motion of (a) a Hoola Hoop or (b) Swirling Liquid in a Glass.

Unlike the wedge in Fig 2, which rotates with the object, the ball in Fig 3 must execute circular motion within the gyrating ring. This relative motion can be detected in the illustration by observing that the ball is in contact with different shaded arc lengths along the gyrating ring as it moves about its circular path of radius D . Thus, a frictional force of the track on the ball needs to be considered. Figure 5 shows the general orientation of the normal and frictional force on the object, as well as specifying a set of reference angles. It can be said that the ring radius, R , lags the gyration radius, r , by the phase angle $\theta (= \psi - \varphi)$.

Thus far, the discussion has been limited to a circular slingatron track. However, such a configuration poses the practical problem of designing a mechanical gate to release the projectile after it reaches the sought after speed, e.g., earth-to-space “escape” velocity. For this reason, an open-ended spiral slingatron is a more feasible projectile-launching track geometry.

Making the conceptual transition from a circular to a spiral slingatron is facilitated by viewing a spiral that is composed of interconnected semicircular arc lengths, Fig 6(a). At any given location, the track is moving within a gyrating circular path, as it was in Fig 5. Here, however, the radius of the circular arc changes every half-revolution, so that an object moving within the launch tube must accelerate in order to complete one revolution in phase with gyrating track, Fig 6(b). Thus, it is conceivable that (under the right normal and friction force conditions) the object can accelerate, even if the period of gyration is constant.

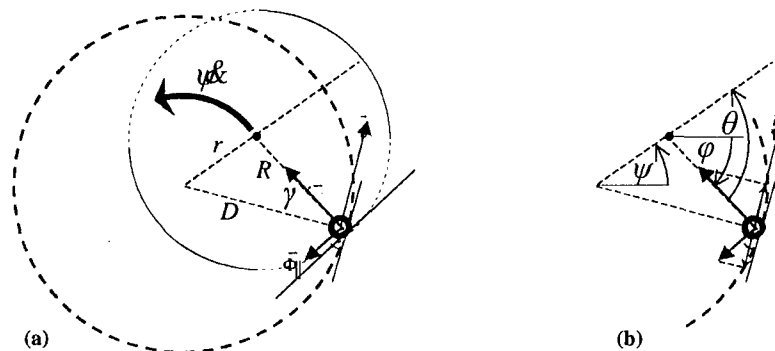


FIGURE 5. (a) Normal and Frictional Force, With (b) Tangential Components, of the Ring on the Mass.

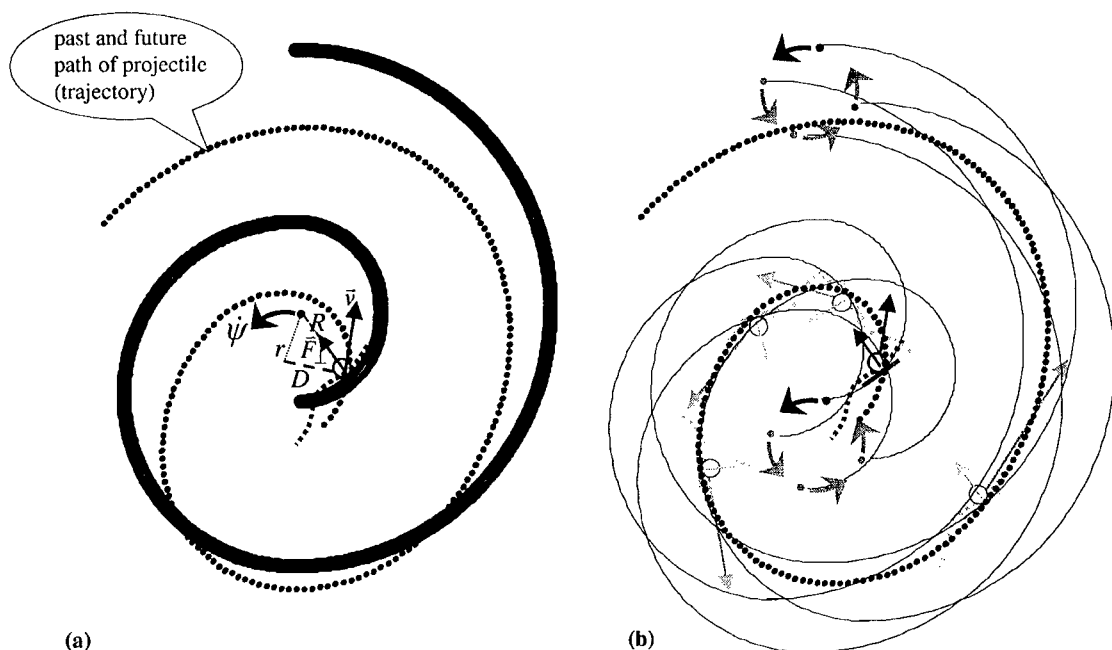


FIGURE 6. Spiral Slingatron, (a) Initial and (b) First Four Quarter-Cycle Gyration Conditions.

EQUATION OF MOTION FOR A SLINGATRON LAUNCHER

The trajectory of the object in Fig 6 is redrawn in Fig 7, with the track and the object in motion suppressed to facilitate visualization of the object's velocity, force, and angular orientation. Unlike the gyrating ring of Fig 5, where the normal force was always directed toward the center of the ring, the direction of the normal force in the gyrating spiral depends on the spiral geometry, $R = R(\phi)$. It can also be characterized by the angle β (Fig 7), defined below. Note that if R does not change with time (or ϕ), the spiral is actually a circle and $\beta = 0$.

$$\beta = \tan^{-1} \left(\frac{\dot{R}}{R\dot{\phi}} \right) = \tan^{-1} \left(\frac{1}{R} \frac{dR}{d\phi} \right) \quad (1)$$

Aided by Fig 7, the x- and y-components of Newton's second law of motion for an object of mass m in the spiral slingatron are:

$$\begin{aligned} m \ddot{x} &= \left| \bar{F}_{\perp} \right| \cos \{ \phi - \beta - \pi \} - \left| \bar{F}_{\parallel} \right| \sin \{ \phi - \beta - \pi \} \\ &= \left| \bar{F}_{\parallel} \right| \sin \{ \phi - \beta \} - \left| \bar{F}_{\perp} \right| \cos \{ \phi - \beta \} \\ m \ddot{y} &= \left| \bar{F}_{\perp} \right| \sin \{ \phi - \beta - \pi \} + \left| \bar{F}_{\parallel} \right| \cos \{ \phi - \beta - \pi \} \\ &= - \left| \bar{F}_{\perp} \right| \sin \{ \phi - \beta \} - \left| \bar{F}_{\parallel} \right| \cos \{ \phi - \beta \} \end{aligned} \quad (2)$$

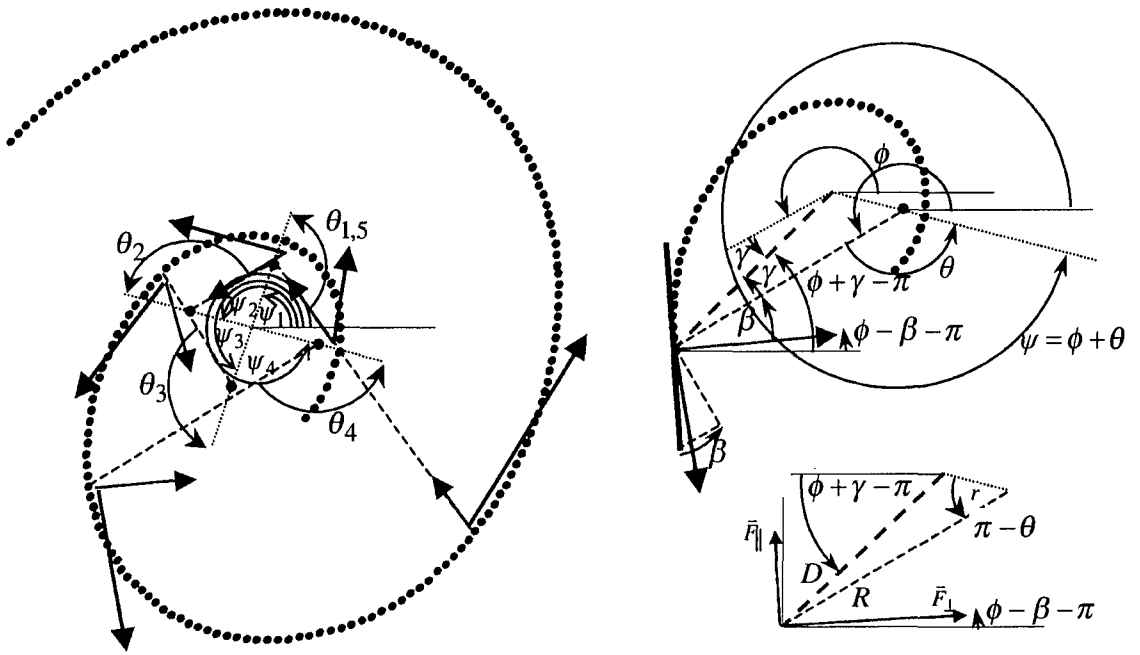


FIGURE 7. Kinematics of a Spiral Slingatron Trajectory.

In general, the force parallel to the track is not only due to track friction, but air friction/drag as well; therefore, assume that

$$|\vec{F}_{\parallel}| = \mu |\vec{F}_{\perp}| + PA \quad , \quad (3)$$

where μ is the coefficient of friction between the circulating mass (ball) and the gyrating track. P is the average frontal air pressure, and A is the object's frontal cross-sectional area. Using Eq 3 in Eq 2 yields:

$$m \ddot{x} (\sin \{\phi - \beta\} + \mu \cos \{\phi - \beta\}) + m \ddot{y} (\mu \sin \{\phi - \beta\} - \cos \{\phi - \beta\}) = PA \quad . \quad (4)$$

Furthermore, in keeping with the geometry designations of Fig 7, the x and y components of the objects location can be written as

$$x = r \cos \{\psi\} + R \cos \{\phi\} \quad (5)$$

$$y = r \sin \{\psi\} + R \sin \{\phi\}$$

Bearing in mind that r is constant, and $R = R(\phi)$,

$$\ddot{x} = \ddot{\phi} \left[\frac{dR}{d\phi} \cos\phi - R \sin\phi \right] + \dot{\phi}^2 \left[\frac{d^2R}{d\phi^2} \cos\phi - 2 \frac{dR}{d\phi} \sin\phi - R \cos\phi \right] - \ddot{\psi} [r \sin\psi] - \dot{\psi}^2 [r \cos\psi] \quad (6)$$

$$\ddot{y} = \ddot{\phi} \left[\frac{dR}{d\phi} \sin\phi + R \cos\phi \right] + \dot{\phi}^2 \left[\frac{d^2R}{d\phi^2} \sin\phi + 2 \frac{dR}{d\phi} \cos\phi - R \sin\phi \right] + \ddot{\psi} [r \cos\psi] - \dot{\psi}^2 [r \sin\psi]$$

Combining Eq 6 and Eq 4 yields the equation of motion for the spiral slingatron, viz.,

$$\begin{aligned} R \ddot{\phi} [\tan\beta(\mu\cos\beta - \sin\beta) - (\cos\beta + \mu\sin\beta)] \\ + R \dot{\phi}^2 \left[\left(\frac{d\tan\beta}{d\phi} + \tan^2\beta - 1 \right) (\mu\cos\beta - \sin\beta) - 2 \tan\beta (\cos\beta + \mu\sin\beta) \right] \\ + r \ddot{\psi} \begin{bmatrix} \sin\beta \{ \sin(\psi - \phi) - \mu\cos(\psi - \phi) \} \\ - \cos\beta \{ \cos(\psi - \phi) + \mu\sin(\psi - \phi) \} \end{bmatrix} \\ + r \dot{\psi}^2 \begin{bmatrix} \cos\beta \{ \sin(\psi - \phi) - \mu\cos(\psi - \phi) \} \\ + \sin\beta \{ \cos(\psi - \phi) + \mu\sin(\psi - \phi) \} \end{bmatrix} - \frac{PA}{m} = 0 \end{aligned} \quad (7)$$

with β given by Eq 1.* Note, if the spiral collapse into a circle, then $\beta = 0$ and the equation of motion for a circular slingatron becomes,

$$\ddot{\phi}R + \dot{\phi}^2 \mu R + r \ddot{\psi} [\cos(\psi - \phi) + \mu\sin(\psi - \phi)] - r \dot{\psi}^2 [\sin(\psi - \phi) - \mu\cos(\psi - \phi)] + \frac{PA}{m} = 0 \quad (8)$$

In this investigation, the only solutions of interest are those for which the gyration rate is steady, i.e., $\dot{\psi}$ is constant. (It is envisioned that size of the spiral slingatron required for earth-to-space launch will be so massive, that it would be difficult to provide such a large

* With the exception of the pressure term, Eq. 7 agrees with the equation of projectile motion in a gyrating and evacuated spiral launch tube, as derived by D. A. Tidman in his unpublished notes, dated November 11, 1997.

structure with any substantial angular acceleration over the short time period that the projectile traverses the launch tube.) Looking for solutions with $\dot{\psi} = 0$ means the motion of an object in the spiral slingatron will conform to

$$\begin{aligned}
 & R \ddot{\phi} [\tan \beta (\mu \cos \beta - \sin \beta) - (\cos \beta + \mu \sin \beta)] \\
 & + R \dot{\phi}^2 \left[\left(\frac{d \tan \beta}{d \phi} + \tan^2 \beta - 1 \right) (\mu \cos \beta - \sin \beta) - 2 \tan \beta (\cos \beta + \mu \sin \beta) \right] \\
 & + r \dot{\psi}^2 \left[\begin{array}{l} \cos \beta \langle \{ \sin(\psi - \phi) - \mu \cos(\psi - \phi) \} \equiv \{ \sin(\theta) - \mu \cos(\theta) \} \rangle \\ + \sin \beta \langle \{ \cos(\psi - \phi) + \mu \sin(\psi - \phi) \} \equiv \{ \cos(\theta) + \mu \sin(\theta) \} \rangle \end{array} \right] - \frac{PA}{m} = 0
 \end{aligned} \quad (9)$$

Clearly, this differential equation of motion is non-linear. A numerical solution is the only one possible. To this end, the numerical integration techniques within Matlab and Simulink (both marketed by Mathworks Inc.) are used here to solve the problem. However, before invoking these solution algorithms, both μ and P need further clarification. For simplicity, the straightforward analytical expression given in Eq 10[†] will be used for the average frontal pressure on the object in the slingatron, viz.,

$$P = \frac{P_{\infty} \gamma (\gamma + 1) M^2}{2} \quad (10)$$

Here, M is the Mach number of the projectile through the air ahead of it, in which the gas pressure is P_{∞} , $\gamma = 1.4$, and the sound speed is 335 m/s. Under these conditions, it was found that air drag can significantly retard the acceleration of the projectile, unless the launch tube is partially evacuated. Since this study is primarily interested in finding the range of possible solutions, it was assumed from the outset that the launch tube could be pumped down to a pressure of $P_{\infty} = 0.01 \text{ atm} = 1.01 \times 10^3 \text{ N/m}^2$.

The friction coefficient, μ , is also found to play a significant role in determining the size and speed of the slingatron needed to achieve the requisite earth-to-space escape velocity, assumed here to be 8 km/s. Tidman [6] has obtained experimental data on μ for speeds up to 2 km/s; a curve fit to that data yielded Eq 11. Until a broader range of data can be sampled, Eq 11 will be utilized to compute μ as a function of the object's velocity.

$$\mu = \frac{0.12}{1.0 + 2.43 \times 10^{-3} |\bar{v}|} \quad (11)$$

[†] This expression can be derived from Equation 3.5, page 64, of Liepman and Roshko [5], in the limit of $P/P_{\infty} \gg 1$, i.e., high object/projectile velocity.

SOLVING THE EQUATION OF MOTION

Spiral Slingatron Parameters

Since $\dot{\psi}$ is the angular rate at which the spiral track gyrates, it is not a variable, but rather, a parameter of the problem. Likewise, the radius of gyration, r , is a parameter, as is the mass, m , and cross-sectional area, A , of the projectile. Depending on the geometry of the spiral, its description can involve several parameters, for instance, a circle requires one parameter—the radius. For simplicity, a two-parameter Archimedes spiral is assumed here, of the form

$$R(\phi) = a\phi + R_0 \quad , \quad (12)$$

where a and R_0 are the two parameters. Initial conditions are also needed to specify the starting angles, ψ_0 and ϕ_0 , as well as $\dot{\phi}_0$. Thus, in total, there are 9 parameters that need to be specified in order to unambiguously solve Eq 9. However, not all of these parameters are varied in this exploratory investigation. In particular, ϕ_0 is taken to be a constant, thereby defining a reference axis; also, the mass m is taken to be a constant, as is the projectile's cross-sectional area A . Furthermore, it is assumed that $\dot{\phi}_0$ is the same as $\dot{\psi}$, i.e., there is no initial time rate of change in the phase angle, θ . Hence, the number of parameter that will be varied in this study is reduced from 9 to 5.

Solution Results

Although a large range of solutions will ultimately be explored, a small subset is chosen first, in order to demonstrate that some parameters have more influence on the solution than others. With this in mind, the initial range of parameters is taken to be:

$$\left. \begin{aligned} \dot{\psi} &= \frac{7\pi}{2}, \frac{9\pi}{2}, \frac{11\pi}{2} \text{ rad/s} & r &= 7.5, 9.5, 11.5 \text{ m} \\ \dot{\phi}_0 &= \dot{\psi} & R_0 &= r+8, r+10, r+12 \text{ m} \\ \psi_0 &= \frac{\pi}{8}, \frac{\pi}{10}, \frac{\pi}{12} \text{ rad} & a &= 0.175 \times r, 0.225 \times r, 0.275 \times r \text{ m} \\ \phi_0 &= 0 \text{ rad} & \theta_0 &= \frac{\pi}{8}, \frac{\pi}{10}, \frac{\pi}{12} \text{ rad} \\ m &= 1,000 \text{ kg} & A &= 0.086 \text{ m}^2 \end{aligned} \right\} \quad , \quad (13)$$

A command procedure was written (containing a series of nested loops), whereby the computed Simulink solution of Eq 9 (using Eqs 1, 10, and 11, for β , P and μ , respectively) is obtained for each of the 243 combinations of parameters/initial conditions set out in Eq 13. A solution for $\phi(t)$ was considered acceptable, for the purpose of launching a projectile into space, if the computed value of the projectile's speed within the spiral track, viz.,

$$\begin{aligned}
 |\vec{v}| &= \sqrt{\dot{x}^2 + \dot{y}^2} \\
 &= \dot{R}^2 + (r\dot{\psi})^2 + (R\dot{\phi})^2 + (2\dot{\psi}\dot{\phi}Rr)\cos\theta - (2\dot{\psi}\dot{R}r)\sin\theta \\
 &= (\dot{\phi}a)^2 + (r\dot{\psi})^2 + ([a\dot{\phi} + R_0]\dot{\phi})^2 + (2\dot{\psi}\dot{\phi}r[a\dot{\phi} + R_0])\cos\theta - (2\dot{\psi}\dot{\phi}ar)\sin\theta
 \end{aligned} \tag{14}$$

reached 8 km/s, at any time. Out of the 243 solutions, only 90 produced a projectile speed of at least 8 km/s. One such solution,

$$\begin{aligned}
 \dot{\psi} &= \frac{11\pi}{2} \text{ rad/s} & r &= 5.5 \text{ m} \\
 \dot{\phi}_0 &= \dot{\psi} & R_0 &= r+12 \text{ m} \\
 \left. \begin{aligned} \psi_0 &= \frac{\pi}{12} \text{ rad} \\ \phi_0 &= 0 \text{ rad} \end{aligned} \right\} \theta_0 &= \frac{\pi}{12} \text{ rad} & a &= 0.275 \times r \text{ m} \\
 m &= 1,000 \text{ kg} & A &= 0.086 \text{ m}^2
 \end{aligned} \tag{15}$$

yielded the results shown in Fig 8.

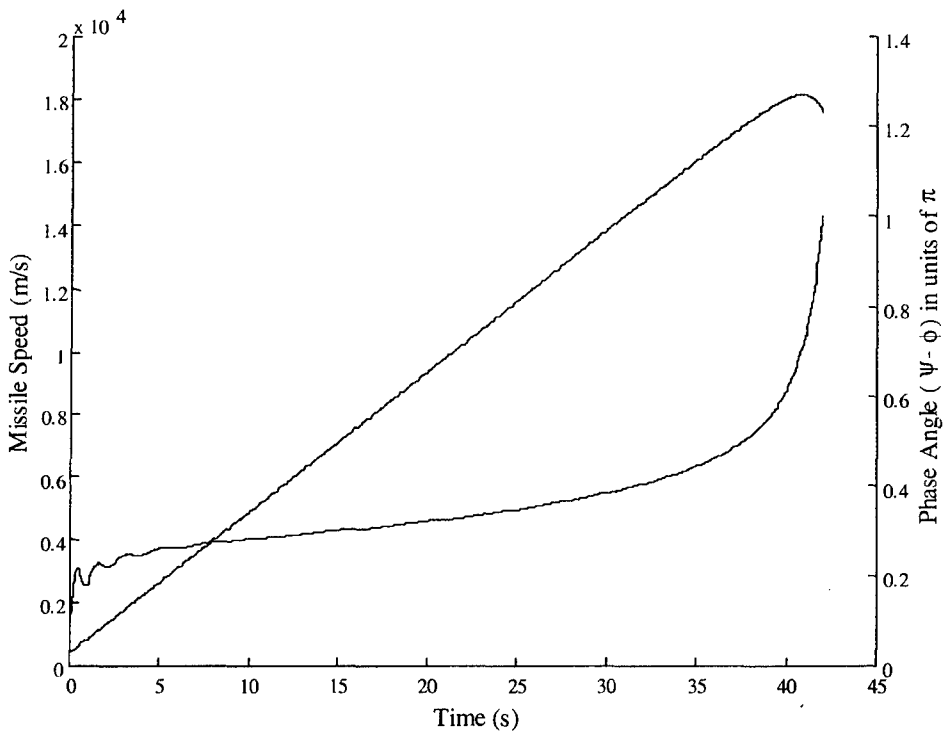


FIGURE 8. Velocity and Phase Angle vs. Time, Based Upon the Simulink Solution of Eq (9) for the Conditions of Eq 15.

It appears from Fig 8 that the solution for the missile's speed, Eq 14, increases in a near-linear fashion, almost independent of the phase angle, $\theta = \psi - \phi$, until such a time (~ 40 s) that the phase angle exceeds some critical value, here $\sim 0.6 \pi$ rad (~ 108 deg), above which it grows rapidly while the speed declines. However, the decline in speed in this case occurs well above the sought after launch velocity of 8 km/s, which requires ~ 17 s for this particular set of slingatron parameters. Figure 9 plots the acceleration of the projectile in the tangent and normal directions to the spiral. Although it is the non-zero tangential acceleration that gives rise to the speed increase in Fig 8, it can be seen that this component is minor in comparison to the acceleration that the projectile undergoes in the direction normal to the track (e.g., ~ 100 g's vs. $\sim 14,000$ g's at the time the projectile reaches 8 km/s).

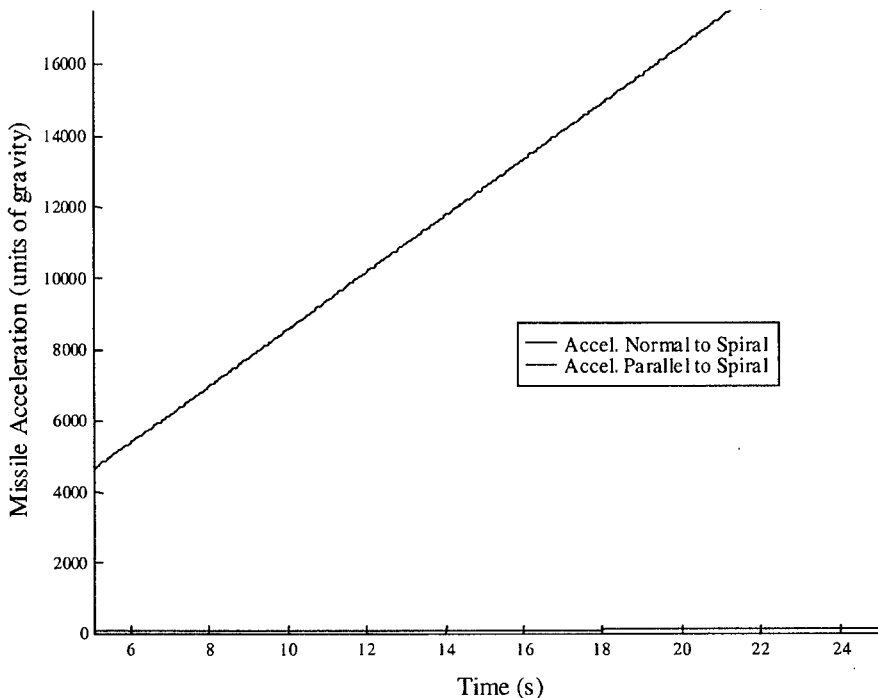


FIGURE 9. Acceleration vs. Time, Based Upon the Simulink Solution of Eq (9) for the Conditions of Eq 15.

The high acceleration of the projectile normal to the track requires a large normal force, creating a substantial wall pressure, displayed in Fig 10. In practice, a track formed from steel pipe would require a considerable wall thickness to accommodate this level of pressure. A finite element model was formulated to analyze the problem. In particular, a time varying pressure load was swept across one side (180 degrees) of the inner surface of a steel tube, Fig 11, assumed to be hinged at both ends. A plot of the peak hoop (circumferential) stress in the tube as a function of wall thickness is shown in Fig 11, for various pipe thicknesses. For example, if a wall pressure of 10 ksi was required to change the projectile's direction in the spiral track, then it would generate a peak inner surface hoop stress of $\sim 6-7$ ksi in a 2 in thick wall. (For reference, 70 ksi is considered a safe hoop-stress level in gun barrel steels.) In the pressure vessel industry, a simple rule of thumb for gauging wall thickness is (Dorf [7]):

$$\text{Wall Thickness (in)} = \frac{\text{Applied Normal Pressure (psi)} \times \text{Inside Cylinder Radius (in)}}{\text{Allowable Stress (psi)} - 0.6 \times \text{Applied Normal Pressure (psi)}} \quad (16)$$

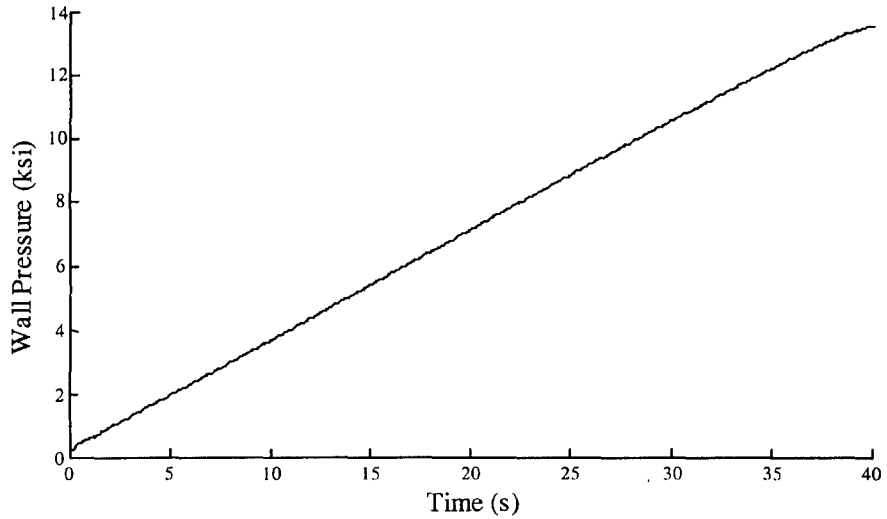


FIGURE 10. Projectile-Track Interface Pressure vs. Time, Based Upon the Simulink Solution of Eq (9) for the Conditions of Eq 15.

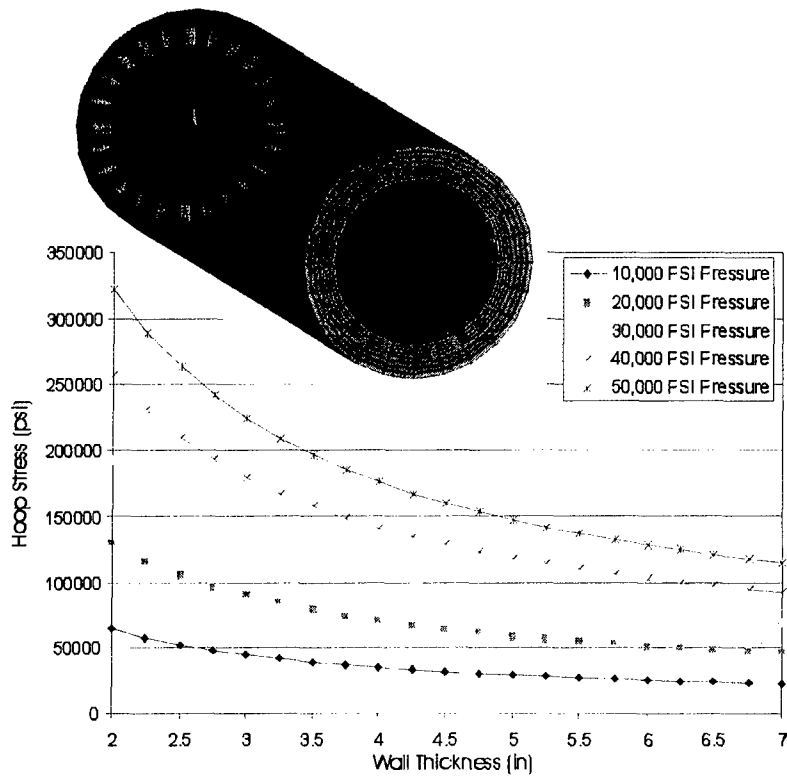


FIGURE 11. Peak Inner Surface Hoop Stress vs. Wall Thickness, for Various Semi-Circular, Inner-Wall Pressure Loadings, in AISI 4340 Steel Pipe.

In order to compute the total weight of a Slingatron track, the total track length needs to be determined. Figure 12 shows the cumulative arc (track) length vs. time for the same Simulink solution as that of Figs 8–11. At 17 s (~8 km/s) the spiral length is ~ 43 mi. Although not shown here, wall pressure vs. track length could also be resolved from the Simulink solution. Similarly, assuming a pipe-like track design made from steel that can safely tolerate a hoop stress of 70 ksi, with inner diameter (from A in Eq 15) of 25 in (0.64 m), Eq 16 can be invoked to provide wall thickness vs. arc length. It was thus determined, that 43 mi of track would weight ~17,000,000 lbs, or, 8,500 tons.

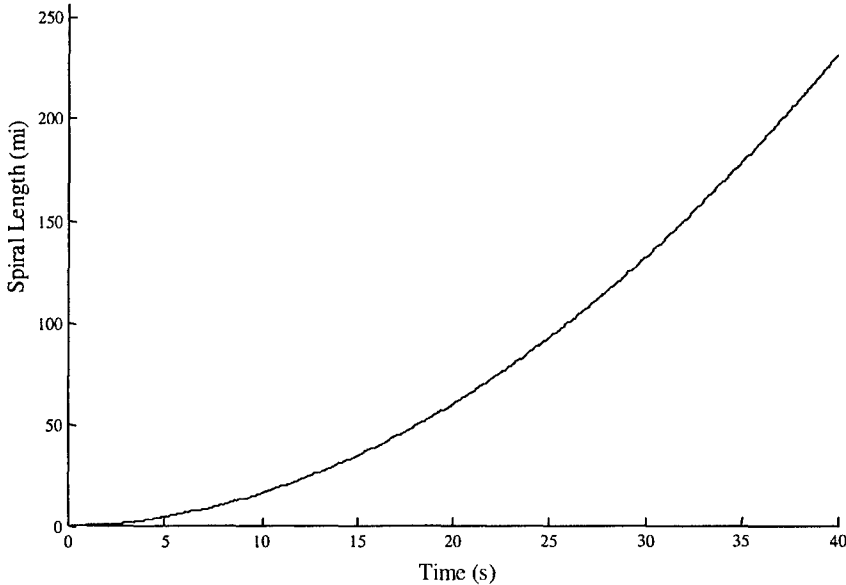


FIGURE 12. Track Length vs. Time, Based Upon the Simulink Solution of Eq (9) for the Conditions of Eq 15.

Upon closer inspection, it was noticed that within the 90 parameter-sets that yielded successful solutions, variation in θ_o and R_o did not strongly affect the outcome. To illustrate this, Fig 17 plots solutions derived from the following subset of Eq 13,

$$\psi = \frac{11\pi}{2} \text{ rad/s} \quad ; \quad \dot{\phi}_o = \psi \quad ; \quad r = 5.5 \text{ m} \quad ; \quad R_o = r + 12 \text{ m}$$

$$a = 0.275 \times r \text{ m} \quad ; \quad m = 1,000 \text{ kg} \quad ; \quad A = 0.086 \text{ m}^2 \quad . \quad (17)$$

$$\left. \begin{array}{l} \psi_o = \frac{\pi}{8}, \frac{\pi}{10}, \frac{\pi}{12} \text{ rad} \\ \phi_o = 0 \text{ rad} \end{array} \right\} \theta_o = \frac{\pi}{8}, \frac{\pi}{10}, \frac{\pi}{12} \text{ rad}$$

As indicated, these three cases differ from each other only by the initial phase angle θ_o .

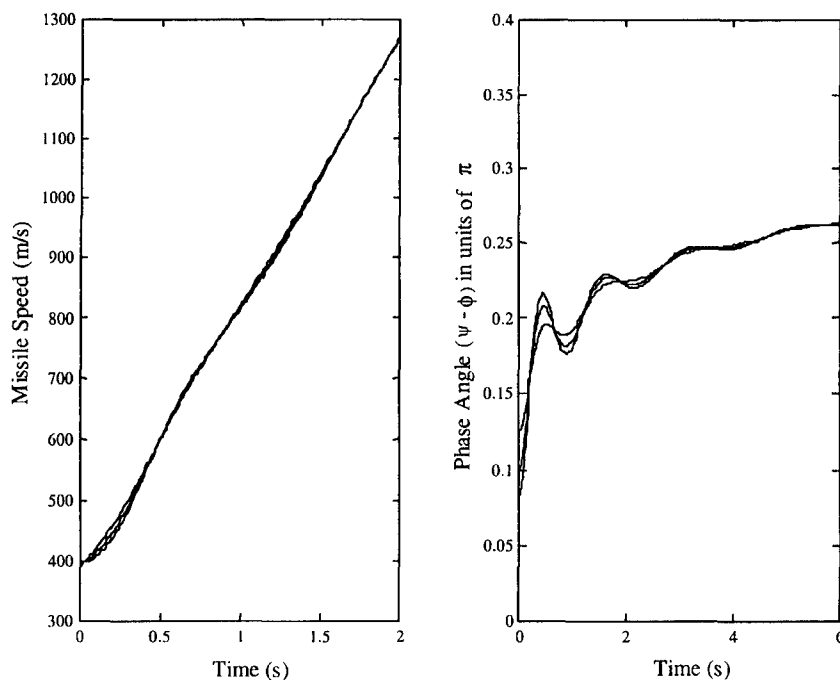


FIGURE 13. Speed and Phase Angle vs. Time, Based Upon the Simulink Solution of Eqs (9) and (17).

As can be seen from Fig 13, variation in the phase angle dampens out, as did its effect on the solution for the projectile's speed. Likewise, though not plotted here, variation in phase angle did not produce significant changes in the total track length, nor did it noticeably affect the plot of wall pressure vs. time. A similar result was found to hold for variation in R_o , viz., significant changes in the initial spiral radius produced insignificant change, over time, in the projectile speed, track length, and wall pressure.

In summary, of the 243 parameter-sets specified in Eq 13, only 90 yielded a solution that produced a projectile speed of 8 km/s (or more). Of these 90, there was a subset of 10 that yielded notably different values for the track length and wall pressure; for each of these 10, there were 9 variations in θ_o or R_o that only slightly perturbed the length and pressure profiles.

In addition to track length and wall pressure, another factor that must be considered in evaluating a practical slingatron design would be the speed at which the spiral track gyrates. For instance, the higher the frame speed, the more energy is expended doing work against air resistance/drag. Furthermore, the higher the structural speed, the higher the loads on moving parts (e.g., bearings) and the more wear and maintenance that can be expected. Figure 14 plots the frame speed vs. wall pressure and track length for the 90 successful launch solutions of Eq 9. The inset plot shows the 10 most unique solutions, demonstrating that variation in θ_o and R_o is not needed to capture the gross range of solutions.

The most desirable solution is the one that has a low track speed, low wall pressure, and short track length; not surprisingly, concurrent minimums in these three parameters appears unachievable. Thus, a compromise has to be made, two of the three desirable traits must be favored at the expense of the third, or, less than minimum values must be accepted for all three factors. For example, from Fig 14, if a maximum wall pressure at projectile exit of 6 ksi could be tolerated, then a minimum spiral length of 43 mi, gyrating at a minimum circular speed of 95 m/s could be achieved. On the other hand, if the maximum wall pressure was set

at 5 ksi, it would necessitate a minimal spiral length of 66 mi with a frame speed of 78 m/s. Also shown in Fig 14 are three solutions where the pressure is 5 ksi and the frame speed is 78 m/s, but the track lengths are vastly different, at 66 mi, 80 mi, and 102 mi, respectively. Although these three designs accomplish the same effect (viz., launching the projectile at 8 km/s), the difference in their costs (one being 40% shorter than the other) would be tremendous; thus proving the potential benefit of this type of parametric analysis.

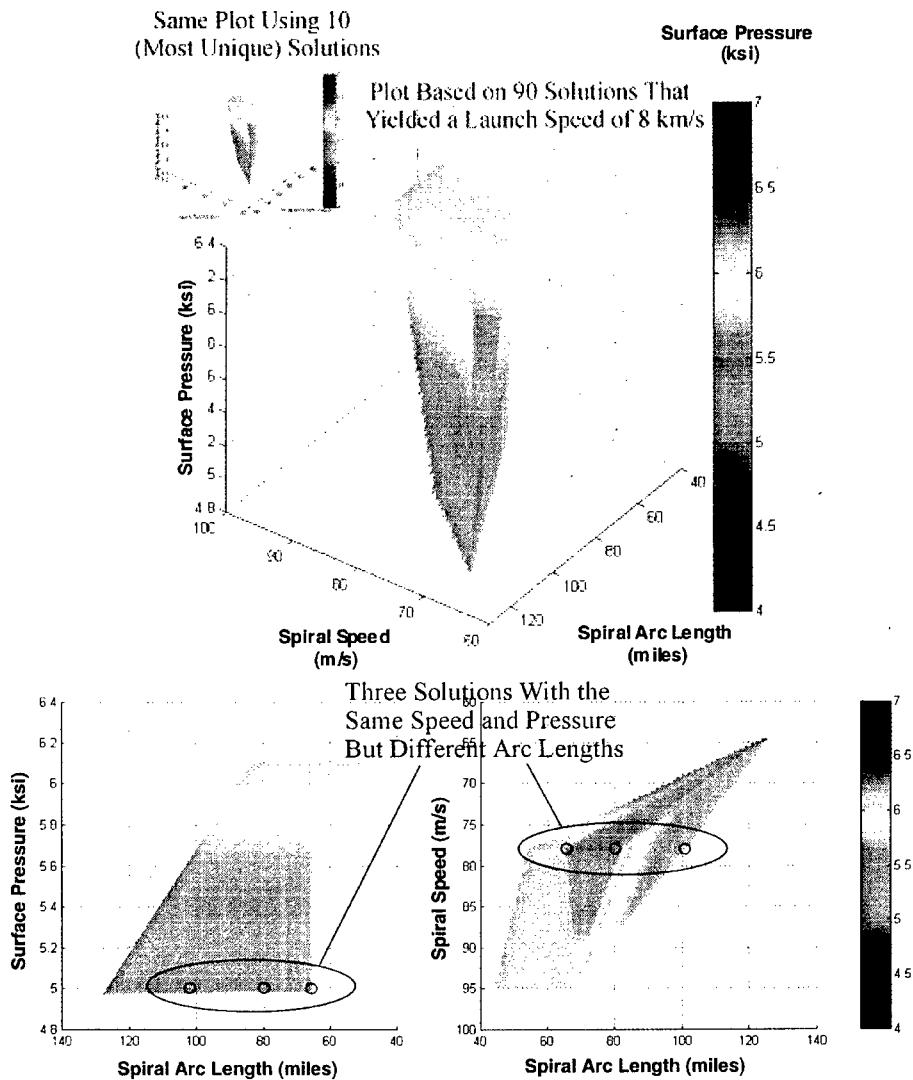


FIGURE 14. Wall Pressure vs. Spiral Speed vs. Spiral Track Length, Based Upon Es (9) and (13).

The relatively small range of parameters specified in Eq 13 has been used to demonstrate (via Figs 8–14) the methodology by which Simulink can be utilized to search for favorable solutions to the problem of a slingatron-based earth-to-space projectile launch, from an engineering-practical vantage point. Although Fig 14 shows a solution surface, the range of parameters upon which it was derived, viz., Eq 13 (with its 243 possibilities), is not all-inclusive. Are there other parameter sets that might produce even better (easier to produce and

maintain) solutions/designs? To answer this question, a broader range of parameters needs to be examined. In order to explore the widest possible range of solutions with the minimum computer time and resources, it is sensible to distribute the collection of parameters in accordance with their degree of influence on the solution. As indicated by the likeness of the 10-solution subset to the full 90-solution assembly in Fig 14, variation in the parameters θ_o and R_o does not produce significantly different results. Therefore, it makes sense to narrow the range of these two parameters and widen the range for the remaining three, viz., the gyration speed parameter, $\dot{\psi}$, the gyration radius, r , and the parameter governing the tightness of the spiral, a . Accordingly, the 18,375 parameter-sets of Eq 18 were examined and (as will be shown) found to yield a range of solutions that liberally bound the region of practical interest.

$$\begin{aligned}
 \dot{\psi} &= \frac{\pi}{2} (2n_1 - 1) \text{ rad/s} ; \text{ for } n_1 = 1:35 & R_o &= r + 4 \text{ m} \\
 r &= n_2 - 0.5 \text{ m} ; \text{ for } n_2 = 1:35 & \dot{\phi}_o &= \dot{\psi} \\
 a &= (n_3 - 0.5) \times 0.05 \times r \text{ m} ; \text{ for } n_3 = 1:15 & m &= 1,000 \text{ kg} \quad , \quad (18) \\
 \left. \begin{aligned} \psi_o &= \frac{\pi}{40} \text{ rad} \\ \phi_o &= 0 \text{ rad} \end{aligned} \right\} \theta_o &= \frac{\pi}{40} \text{ rad} & A &= 0.086 \text{ m}^2
 \end{aligned}$$

Out of the 18,375 different combinations of parameters, there were 16,178 successful solutions (of Eq 13 for $\phi[t]$) that yielded a projectile speed (Eq 14) of at least 8 km/s. Fig 15 is the counterpart of Fig 14, displaying all 16,178 solutions.

Clearly, a structural speed that is greater than the speed of sound (~ 335 m/s) is impractical, neglecting these cases would eliminate the majority of the solutions indicated in Fig 15. A more reasonable speed might be several hundred meters per second slower. Searching the solution set, Fig 16 shows a subset plot of 600 solutions where the structural speed of the track was < 140 m/s and the track length is $< \sim 100$ mi.

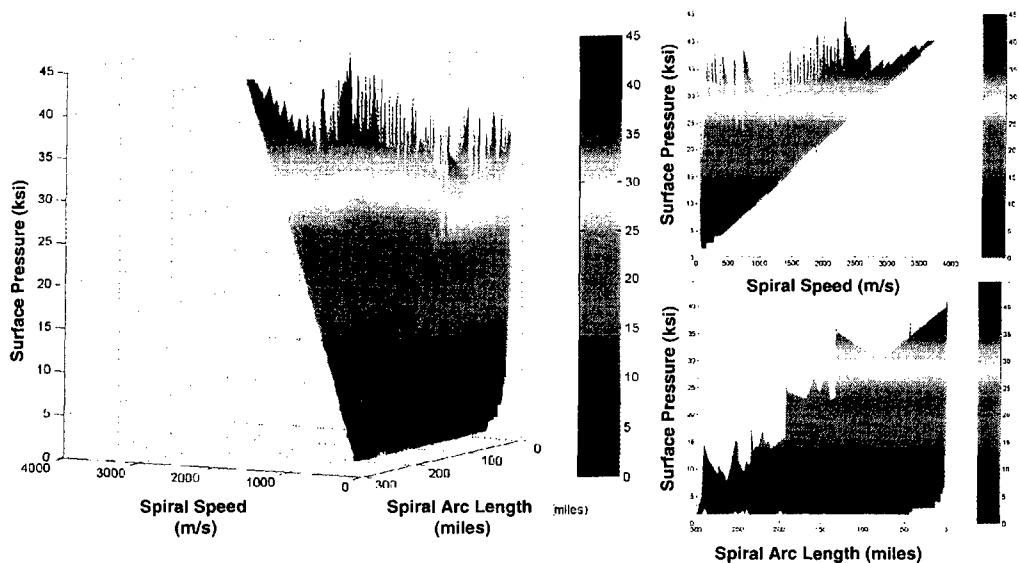


FIGURE 15. Wall Pressure vs. Spiral Speed vs. Spiral Track Length, Based Upon Eqs (9) and (18).

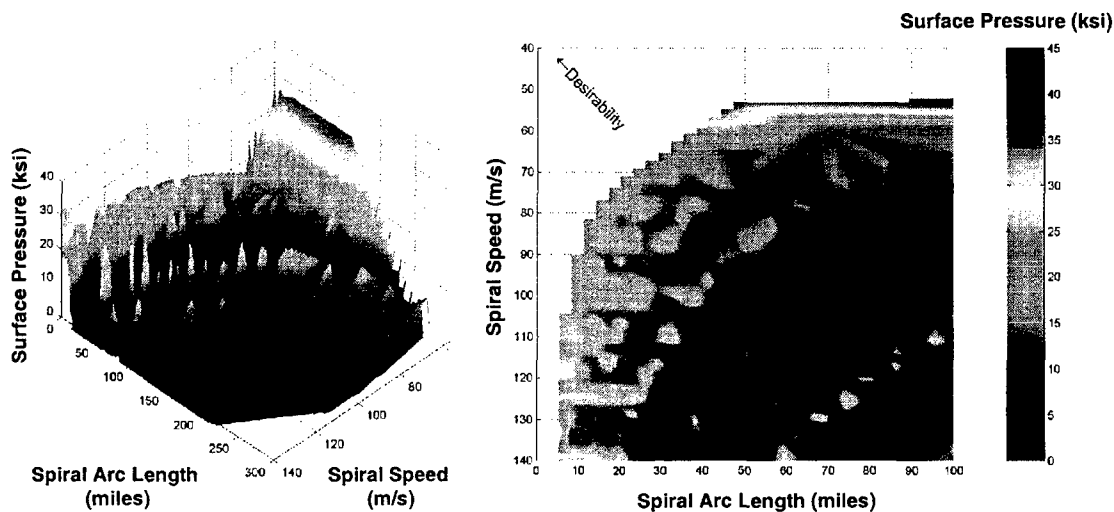


FIGURE 16. Wall Pressure vs. Spiral Speed vs. Spiral Track Length, Based Upon Eqs (9) and (18).

At the upper speed end in this subset is a solution ($n_1 = 2$, $n_2 = 30$, $n_3 = 13$) where the structure is moving at 139 m/s (313 mph), the peak wall pressure is below 2 ksi, and the track length is a, relatively, moderate 54 mi. Based on the same approach used to determine the 8,500-ton track weight in the previous (95-m/s, 6-ksi, 43-mi) example, this designated-upper-speed-limit, 54-mi track would weigh a relatively low 2,700 tons.

At the low speed end, a solution exists ($n_1 = 34$, $n_2 = 1$, $n_3 = 2$) where the track motion is slowed down to 53 m/s; the track length remains in the middle ground at 48 mi, but the wall pressure peaks at 37 ksi. The estimated weight of this lower-speed-limit track is high, at 107,000 tons.

A more all-around-moderate solution ($n_1 = 7$, $n_2 = 4$, $n_3 = 6$) would have the track moving at 72 m/s, with a wall pressure of 7 ksi, and a track length, again in the mid-range, at 50 mi. The estimated weight of this track would be 12,200 tons.

Perhaps the best solution compromise for structural speed, peak wall pressure, length, and weight is one ($n_1 = 10$, $n_2 = 3$, $n_3 = 7$) that produces mid-range values for the frame speed, at 75 m/s (170 mph), wall pressure, at 11 ksi, weight, at 10,500 tons, and a low-end track length of 28 mi. (For reference, this slingatron would be the weight-motion equivalent of two fully-loaded medium-sized river barges, each circling at ~5 hz around an ~8 ft radius.)

Although the evidence is anecdotal, the values for n_1 , n_2 , and n_3 in the four practical-solution examples described above and tabulated below (spanning the high, moderate, and low frame speed regimes) illustrate that the range of n_1 and n_2 , from 1–35, and n_3 , from 1–15, was broad enough to capture the majority, if not all, of the most practical slingatron designs.

SUMMARY

This report provides a physical explanation of the mechanism by which the mechanical device, referred to as a slingatron, akin to a hoola-hoop, can be used to launch a projectile into space. Furthermore, using the software program called Simulink (a complementary program to Matlab) the non-linear differential equation of motion for a spiral slingatron design was solved

for a large range of input parameters. These solutions were sorted based upon whether or not the slingatron design could accelerate a 1000-kg, 0.64-m diameter projectile to at least 8 km/s (assumed to be a sufficient speed to place such a payload into space). Finally, the most physically reasonable of these successful solutions were down-selected. A case in point, it was found that a spiral track 28 mi long weighting 10,500 tons having a structural speed of ~170 mph could be used to launch such a projectile into space.

With the type of information provided in this study (viz., structural speed, wall pressure, and track length), a more detailed track-design analysis could begin, leading to, among other things, a total-dollar (or per-payload-pound) cost estimate for a slingatron-based earth-to-space launch system.

Table 1. Examples of the “Most Practical/Optimum” Slingatron Track Designs

Minimum Values	Structural Speed (m/s)	Wall Pressure (ksi)	Track Length (miles)	Weight (U.S. tons)
A	139	2	54	2,700
B	53	37	48	107,000
C	72	7	50	12,200
D	75	11	28	10,500

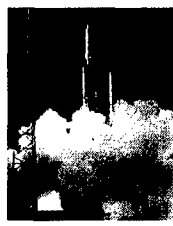
500-ft Fully Loaded Cargo Ship—8,000 tons



Large Steel River Bridge—10,000 tons



Titan IV Rocket—340-380 tons



1000-ft Fully Loaded Aircraft Carrier—80-100,000 tons



Golden Gate Bay Bridge—200,000 tons



International Space Station—520 tons



REFERENCES

- [1] Tidman, D. A., R. L. Burton, D.S. Jenkins, and F.d. Witherspoon. “Sling Launch of Materials into Space.” *Proceedings of 12th SSI/Princeton Conference on Space Manufacturing*, ed. By B. Faughnan, Space Studies Institute, Princeton, NJ, pp 59–70, May 4–7, 1995.
- [2] Tidman, D. A. “Sling Launch of a Mass Using Superconducting Levitation.” *IEEE Transactions on Magnetics*, vol. 32, no. 1, pp 240–247, January, 1996.
- [3] Tidman, D. A. “Slingatron Mass Launchers.” *Journal of Propulsion and Power*, vol. 14, no. 4, pp 537–544, July–August, 1998.
- [4] Tidman, D. A. and J. R. Greig. “Slingatron Engineering and Early Experiments.” *Proceedings of the 14th SSI/Princeton Conference on Space Manufacturing*, ed. By B. Faughnan, Space Studies Institute, Princeton, NJ, pp 306–312, May 6–9, 1999.
- [5] Liepman, H. W., and A Roshko. “Elements of Gasdynamics.” John Wiley & Sons, Inc., New York, Eq 3.5, page 64, 1957.
- [6] Tidman, D. A. “The Spiral Slingatron Mass Launcher.” *Proceedings of the 10th U.S. Army Gun Dynamics Symposium*, April 23-26, 2001.
- [7] Dorf, R. C. “The Engineering Handbook.” CRC Press Inc, Boca Raton, FL, page 85, 1996.